TEMPERATURE ASSESSMENT OF A VERTICAL MEMBER SUBJECTED TO LOCALISED FIRE

Christophe THAUVOYE[1], François HANUS[2], Olivier VASSART[2], Bin ZHAO[1]
[1]CTICM, Espace technologique l'orme des merisiers, 91190 Saint-Aubin, France
[2]ArcelorMittal Global R&D, 66 rue de Luxembourg, L-4009 Esch sur Alzette, Luxembourg

ABSTRACT

This paper describes the model developed during the European LOCAFI1 project with the aim to assess the temperature of a vertical element subjected to a localised fire in a compartment. This model focuses on the calculation of heat fluxes with a special emphasis on the radiative heat flux which governs the temperature for sections of a vertical member. It is modelled through the concept of virtual solid flame and involves a surface integral. Even if it allows a precise estimation of heat fluxes and although it can easily be introduced in a simple and computationally fast program, it remains a complex method. Thus, in a second step the previous model is simplified, leading to an analytical model. Finally, the model with its two refinement levels is validated against the experimental tests and numerical simulations performed in the project.

INTRODUCTION

For building typologies where a generalised fire cannot develop (e.g.: external structures, open car parks, atria, large industrial or transportation halls, etc), localised fires are an important issue. Zone models (either one-zone or two-zone) are not foreseen to incorporate the effects of localised fires on structures. The main challenge for this is the calculation of the thermal profiles in the structural elements as a function of the fire location and the evolution of this fire with time (diameter, fire load density, RHR, etc). Various recent research projects have allowed developing analytical design methods and demonstrated their validity with experimental evidences but a common lack of the existing approaches is the absence of a satisfying calculation model for the temperature field in vertical members. Due to the complexity of the phenomenon, no analytical method has been developed yet and the available methods are time-consuming numerical methods (e.g. Computational Fluid Dynamics).

The current version of EN 1991-1-22 includes an annex dedicated to localised fire where two calculation methods are described. However, none of these two methods enables assessing the thermal attack induced by a localised fire on a vertical member that is not engulfed into the fire. On these premises, the European LOCAFI project was funded with the aim to provide designers a simplified model that will allow them designing steel columns subjected to localised fires. In this paper, the first part is devoted to the description of a new analytical method for the temperature assessment of vertical members. The model, based on the concept of virtual solid flame for the radiative part, was developed with two levels of complexity which are described hereafter. In the last part, the model with its two levels of refinement is validated against both experimental tests and numerical simulations.

DESCRIPTION OF THE MODEL

The model for calculating the temperature of vertical member at a specific height is sub-divided into several steps:

- Flame modelling.
- Radiative heat flux

- Convective heat flux
- Total heat flux
- Vertical member modelling
- Temperature of the element

Flame modelling

The flame produced by a localised fire affects an exposed member mainly through radiative heat flux if the member is not engulfed. In that case, the flame shape and the relative position flame / vertical member have a strong influence over the radiative heat flux. The concept of virtual solid flame is then used, the flame is seen as a "solid" surface that radiates toward the element.

The model assumes that the fire area has a circular shape on the ground. If the main combustible involved in the localised fire is not circular, then it is modelled as a circle assuming that the area on ground is equal. The virtual solid flame is modelled as a cone and, if it impacts the ceiling, the cone is truncated and an additional ring is added (see Figure 1).

Figure 1 : flame shape

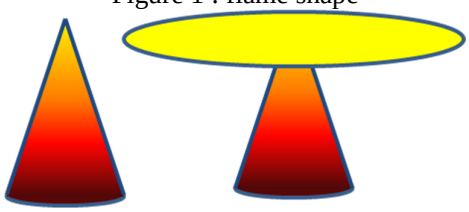

The geometry of the solid flame is fully determined by the cone height. If it does not impact the ceiling, Heskestad3 correlation is used to calculate the height. This correlation, used in the Annex C of EN1991-1-2, is based on the following formula:

$$h_f = -1.02D_{fire} + 0.0148Q(t)^{0.4} \quad [m] \qquad [1]$$

Where D_{fire} [m] is the diameter of the fire source and Q [W] is the heat release rate of the fire source.

The fact that the flame impacts the ceiling or not is determined by comparing the solid flame height h_f to the height under the ceiling h_{ceil}. If h_f is lower than h_{ceil}, the flame does not impact the ceiling. On the other case, it impacts the ceiling.

The temperature of the virtual solid flame varies with height z according to a complementary formula provided in the EN 1991-1-2:

$$\theta_f(z) = \min\left(900; 20 + 0.25\left(0.8Q(t)\right)^{2/3}(z - z_0)^{-5/3}\right) \quad [°C] \qquad [2]$$

The formula is completed by the calculation of the virtual origin z_0:

$$z_0 = -1.02D_{fire} + 0.00524Q(t)^{0.4} \quad [m] \qquad [3]$$

If the flame is impacting the ceiling, the same equations are used to obtain the temperature of the lower part of the flame (i.e. the cone). For the flames spreading under the ceiling, the model is based on Hasemi's method4 in order to calculate the radius of the flame ring. This radius L_h follows:

$$L_h = H\left(2.9Q_h^{0.33} - 1\right) \quad [m] \qquad [4]$$

H is the distance between the fire source and the ceiling.

Q_h, a non-dimensional heat release rate, is estimated through:

$$Q_h = \frac{Q}{1.11\ 10^6 H^{2.5}} \quad [-] \qquad [5]$$

For the ring, the temperature depends on the distance *r* from the centre (*r* is comprised between 0 and L_h) and is derived from Hasemi heat flux taking into account convective and radiative parts using the procedure hereafter.

In a first step, the variable *y* is introduced as:

$$y = \frac{r+H+z'}{L_h+H+z'} \qquad [6]$$

All quantities are already known except for z' which if defined by:

$$z' = 2.4 D_{fire}\left(Q^{*2/5} - Q^{*2/3}\right) si\ Q^* < 1$$
$$z' = 2.4 D_{fire}\left(1 - Q^{*2/5}\right) si\ Q^* \geq 1 \qquad [7]$$

Q^* is as Q_h a non-dimensional heat release rate estimated in a similar way:

$$Q^* = \frac{Q}{1.11\ 10^6 D_{eq}^{2.5}} \quad [-] \qquad [8]$$

Hasemi uses several relations to determine the incident heat flux depending on the value of *y*:

$$\begin{cases} H_s = 100000\ \mathrm{W.m^{-2}} & \text{if } y \leq 0{,}3 \\ H_s = 136300 - 121000.y\ \mathrm{W.m^{-2}} & \text{if } 0{,}3 < y < 1{,}0 \\ H_s = 15000.y^{-3.7}\mathrm{W.m^{-2}} & \text{if } 1{,}0 \leq y \end{cases} \qquad [9]$$

Then, it is divided into two parts assuming that the temperature is linked to the heat flux at this point by the equation:

$$H_s = \varepsilon_f . \sigma . \left(\left(\theta_f + 273\right)^4 - 293^4\right) + h_{conv}\left(\theta_f - 20\right) \qquad [10]$$

σ, the Stefan-Boltzmann's constant, is equal to 5.67 10^{-8} $W.m^{-2}.K^{-4}$. The flame emissivity ε_f is set to 1 in agreement with EN 1991-1-2 hypotheses. h_{conv} is the coefficient of heat transfer by convection which is set to $35 W.K^{-1}.m^{-2}$ as recommended by the Eurocode for simple fire models. Finally, this equation is solved in order to determine θ_f [°C].

Radiative heat flux

In the concept of virtual solid flame, the solid flame is seen as radiative surface. It is divided into several zones referred later as "elementary band", the radiative heat flux received by a face of a vertical member at a specific height is the sum of radiative heat fluxes emitted by each elementary band (see Figure 2).

Figure 2 : radiative exchange between the solid flame and the member

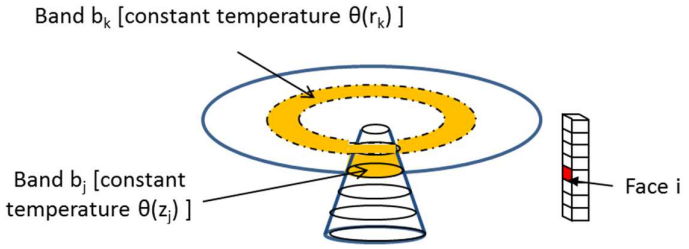

Moreover, the temperature of each elementary band is uniform and the radiative heat flux can be calculated using its temperature and the view factor between this zone and the face i:

$$flux_{flame \to face_i} = \sum_{b_j} \sigma . \varepsilon . \left(\theta_{f,j} + 273\right)^4 . F_{b_j \to face_i} \quad [11]$$

Where ε is the member emissivity, $\theta_{f,j}$ is the temperature of band b_j [°C] and $F_{b_j \to face_i}$ is the configuration factor between band b_j and the elementary face $face_i$ according to the Figure 2.

Considering the band b_j as a radiative surface, the configuration factor $F_{b_j \to face_i}$ is:

$$F_{b_j \to face_i} = \int_{S_{band b_j}} \frac{cos(\theta_1) cos(\theta_2) dS1}{\pi r^2} \quad [12]$$

This factor represents the fraction of the total radiative heat leaving the radiating surface S_{bandbj} which impacts the receiving surface $face_i$. Its value depends on the size of the radiating surface, on the distance from the radiating surface to the receiving surface and on their relative orientation as indicated in Figure 3. It involves a surfacic integral that can be computed through numerical integration but that integral can be reduced to analytical formula when the geometry and the position of the surfaces are simple.

Figure 3 : Radiative heat transfer between emitting and receiving surfaces

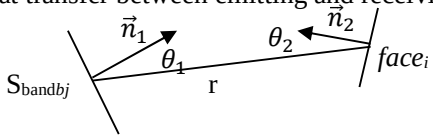

Convective heat flux

As stated previously, the temperature of sections of a member subjected to a localised fire is mainly affected by radiative heat flux as they are surrounded by gases at the ambient temperature. In that case, no additional convective heat flux is added.

Nevertheless, this is not true in the smoke layer that spreads under the ceiling, where the convective heat flux cannot be neglected compared to the radiative heat flux. For a localised fire, the width of the smoke layer is generally small compared to the height of the compartment. If there are some elements that control the smoke spreading under the ceiling, then the smoke layer height h_{smoke_layer} is defined by their geometric characteristic, typically the height of beams.

The temperature of gases surrounding the vertical member is estimated in the same way as for the radiation of flame spreading under the ceiling in order to remain consistent. The first step is the calculation of the heat flux H_s using Hasemi method as described previously and considering r as the distance between the fire center and the vertical member. Then the temperature $\theta_f(r)$ of gases is deduced using the equation where the heat flux Hs is divided into two parts. Finally, the convective heat flux is equal to:

$$\varphi_{conv} = h_{conv}\left(\theta_f(r) - 293\right) \ [\mathrm{W.m^{-2}}] \quad [13]$$

Figure 4 : scheme for the convective heat flux calculation under the ceiling

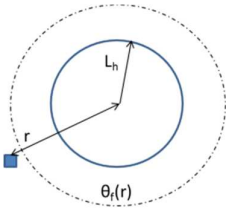

Total heat flux and multiple fire sources

Up to now, only one fire source was taken into account but it is common to have fire scenarios where several sources are involved. The model can handle such situations easily. The radiative heat flux received by any face of the vertical member is just the sum of radiative heat fluxes emitted by each source assuming an upper limit of 100 kW.m^{-2}.

If we consider *n* fire sources:

$$flux_{all\ solid\ flame \to face_j} = \max\left(100000, \sum_{i=1}^{n} flux_{solid\ flame_i \to face_j}\right)\ [\mathrm{W.m^{-2}}] \qquad [14]$$

For the convective part, the heat flux $H_{s,j}$ are calculated using Hasemi's method for each fire source. Then, they are added to give an intermediate heat flux H_s, and again an upper limit of 100 kW.m^{-2} is used.

$$H_s = min\left(\sum_{j=1}^{n} H_{s,j}\ , 100000\right) \qquad [15]$$

Finally, the temperature of hot gases is estimated through equation [10] and the convective heat flux is given by injecting this temperature into [13].

The total absorbed heat flux is the sum of the convective heat flux and the radiative heat fluxes previously calculated with an upper limit set to 100 kW.m^{-2}.

Vertical member modelling

The vertical member is discretised as a succession of sections (at height z_j) where the heat flux is calculated. At this point, it is possible to use the model to compute the heat flux received by the section and thus its temperature using advanced numerical program. It allows handling complex section shapes and specifically the shadow effect when some parts of a section shadows other surfaces from the incident radiation. It was implemented in the F.E.M software SAFIR5 in the framework of the project.

SIMPLIFIED MODEL

One of the project goal is to provide a practical model for designers. So, in a second step, a simplified version of the model is proposed. Two elements are simplified: the vertical member modelling and the virtual solid flame shape in order to replace the surface integral by analytical formulae.

Member modelling

The sections of the vertical member are modelled with a rectangular shape, as indicated in Figure 5, independently of their original shape: I, H or O. This approach is consistent with the assumptions made in the annex G of Eurocode 1 part 1.21. For that rectangular section, the heat flux is determined for the four faces, and then a mean-value is calculated for the whole section by averaging the heat

fluxes of faces by their width.

Figure 5 : H-column modelling and detailed modelling of a section

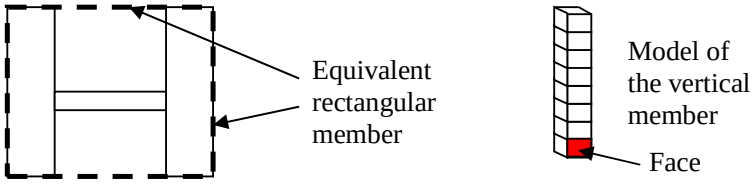

Solid flame modelling

For simple geometrical shapes, analytical formulae exist for the configuration factor. Such formula exists for cylinders and rings. The conical shape is approximated as a succession of cylinders and rings using the equations of the first part to determine their properties (see Figure 6).

Figure 6 : simplified flame shape

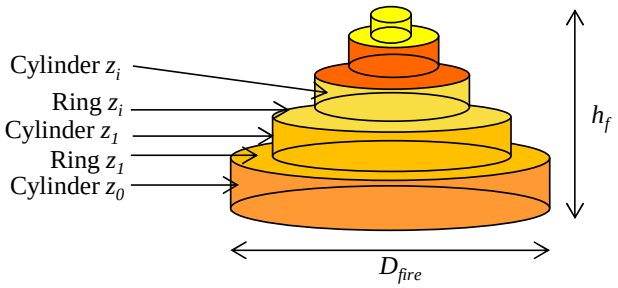

- The configuration factor between an infinitesimal plane and a finite cylinder follows6:

$$F_{dA_1 \to A_2} = \frac{S}{B} - \frac{S}{2B\pi}\left\{\begin{array}{c} cos^{-1}\left(\frac{Y^2-B+1}{A-1}\right) + cos^{-1}\left(\frac{C-B+1}{C+B-1}\right) \\ -Y\left[\frac{A+1}{\sqrt{(A-1)^2+4Y^2}} cos^{-1}\left(\frac{Y^2-B+1}{\sqrt{B}(A-1)}\right)\right] \\ -\sqrt{C}\frac{C+B+1}{\sqrt{(C+B-1)^2+4C}} cos^{-1}\left(\frac{C-B+1}{\sqrt{B}(C+B-1)}\right) \\ +H cos^{-1}\left(\frac{1}{\sqrt{B}}\right) \end{array}\right\} \quad [-] \qquad [16]$$

With $S = s/r, X = x/r, \mathrm{Y} = y/r, H = h/r, A = X^2 + Y^2 + S^2, B = S^2 + X^2, C = (H - Y)^2$

Figure 7 : Configuration cylinder – plane element

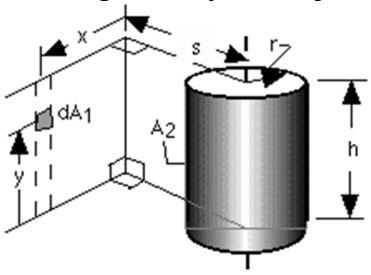

The radiative heat flux received and absorbed by the face *face*$_j$ from the cylinder z_i is then:

$$flux_{Cylinder\ z_i \to face_j} = \sigma.\varepsilon.\left(\theta_f(z_i) + 273.15\right)^4.F_{Cylinder\ z_i \to face_j} \quad [W.m^{-2}] \qquad [17]$$

Where $F_{Cylinder\ z_i \to face_j}$ is the view factor of the cylinder z_i and the face *face*$_i$ calculated with [16].

Figure 8 : radiative exchange between the cylinder z_i and the face j

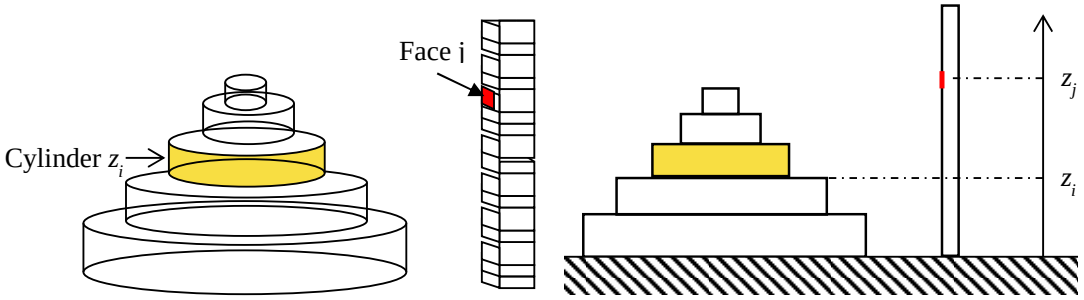

There is a restriction for the application of the formula [16]: the plane cannot cut the cylinder. So additional rules are needed in order to handle all possible configurations. Indeed, in the case shown on Figure 9, the face 1 sees the cylinder, the face 2 and 4 see partially the cylinder while no radiative heat flux from the virtual solid flame reaches the face 3. Thus, the face 1 corresponds to the situation described by the formula [16] and can be handled. For the face 3, the incident radiative heat flux is null. The case of faces 2 and 4 is more complex and the formula cannot be applied directly because the plane (of the face) cuts the cylinder.

Figure 9 : example of cylinder – vertical member interaction (top view)

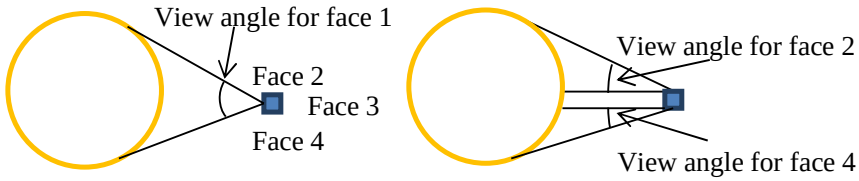

As the radiative heat flux is mainly controlled by the solid angle between the radiative source and the target, the adopted solution is to use a surface shape which will lead to an equivalent configuration factor. A cylinder with a modified geometry (indicated on Figure 10) is used. The diameter of the cylinder is reduced so that the modified cylinder is fully visible by the target face and consequently the analytical formula [16] can be used.

Figure 10 : cylinder modelling

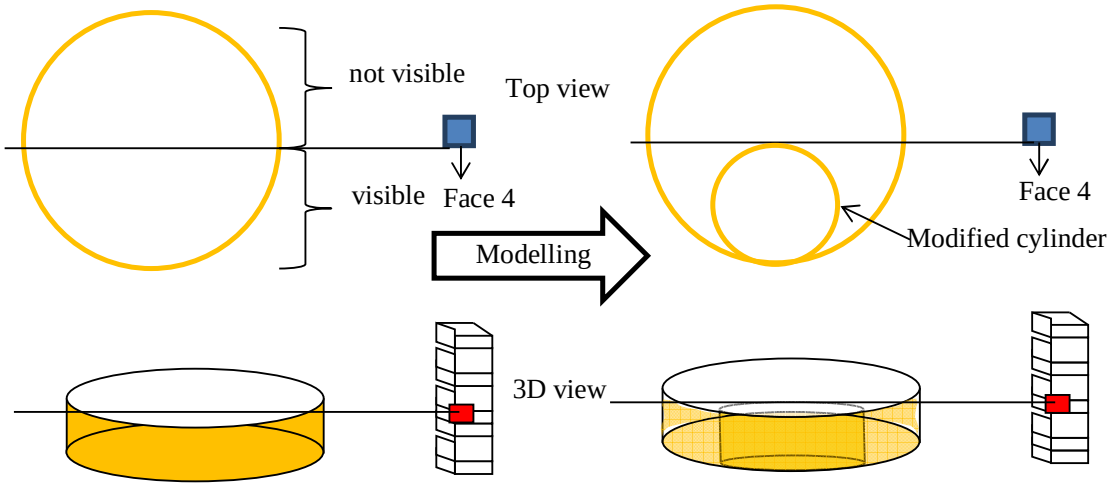

- The configuration factor between an infinitesimal plane element and a ring in a perpendicular plane follows6:

$$F_{dA_1 \to A_2} = \frac{H}{2}\left(\frac{H^2+R_2^2+1}{\sqrt{(H^2+R_2^2+1)^2-4R_2^2}} - \frac{H^2+R_1^2+1}{\sqrt{(H^2+R_1^2+1)^2-4R_1^2}}\right) \quad [-] \qquad [18]$$

With $H = h/l, R = r/l$ and this formula is valid only if $l > r_2$.

Figure 11 : Configuration ring – plane element

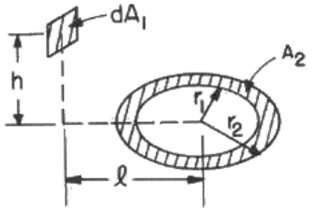

The annular part (ring z_i) between two cylinders is considered as a radiative surface (see Figure 6) and the induced heat flux is computed through [18]. Furthermore, it is added only if the considered section height z_j is greater than the height of the ring z_i (the face "sees" the ring).

As for cylinders, additional rules need to be applied in order to handle all possible configurations. Theoretically, it is valid only for a ring centred in a plane perpendicular to the target, which is not always true. The second point which has a strong impact on the heat flux exchanged by two surfaces is their orientation through a cosine (see Figure 12). The analytical formula corresponds to the case where the orientation is normal and gives the highest view factor. In consequence, it is safe sided and the formula [18] remains used with *l* the distance between the face and the ring centre.

Figure 12 : influence of the orientation of the target

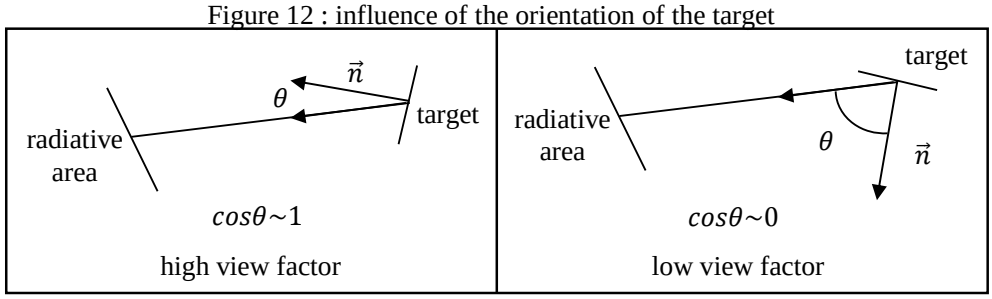

Another point must be taken into account: the ring, as for the cylinder, can be partially visible (see Figure 13). Then, the exterior and even the inner radius of the ring are reduced to give a visible ring in the same way than for a cylinder. In the example presented in Figure 13, the ring defined by its inner radius r_{zi+1} and its outer radius r_{zi}.are both adjusted.

Figure 13 : handling of complex case of ring modelling

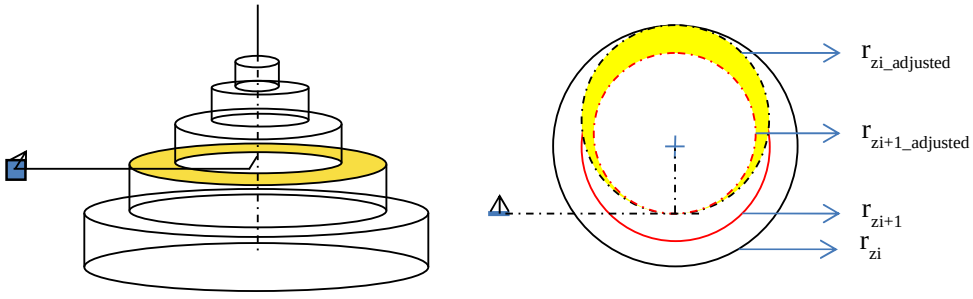

The radiative heat flux received by a face is the sum of the radiative heat flux emitted by all cylinders and rings:

$$flux_{solid\ flame \to face_j} = \sum_i \sigma.\varepsilon.\left(\theta_f(z_i)+273.15\right)^4.F_{Cylinder\ z_i \to face_j} + \sum_i \sigma.\varepsilon.\left(\theta_f(z_i)+273.15\right)^4.F_{Ring\ z_i \to face_j}\ [W.m^{-2}] \quad [19]$$

Then, the mean radiative heat flux over the section at the height z_j is computed by averaging the radiative heat flux over the four faces by the width l_i of each face:

$$flux_{rad_{section}z_j} = \frac{\sum_{i=1}^{4} l_i.flux_{solid\ flame \to face_i}}{\sum_{i=1}^{4} l_i}\ [W.m^{-2}] \quad [20]$$

For sections outside the smoke layer, the convective heat flux remains neglected and the total heat flux absorbed by a section is equal to $flux_{rad_{section}z_j}$.

Furthermore, it was observed that for flames impacting the ceiling, the radiative heat flux induced by the disk (see Figure 1) under the ceiling has an influence limited to a small height. In addition, it is quite difficult to model thus the solution retained in the simplified model is that inside the smoke layer the heat flux absorbed by a section is computed using Hasemi's method (equations [4] to [9]).

Finally, the temperature of a section z_j evolves according to the net heat flux which is the difference between the absorbed heat flux and the emitted heat flux. It is given by the thermal balance heat which is for a homogeneous temperature section:

$$\rho C_p(T)\frac{dT}{dt} = \frac{A_m}{V}\left[Total\_heat\_flux_{section\ z_j} + h_{conv}(20-T) + \varepsilon\left(\sigma(293^4-(T+273)^4)\right)\right] \quad [21]$$

Where ρ, $C_{p,}$ and A_m/V are related to the vertical member properties and respectively its density [kg.m^{-3}], its specific heat [J.kg^{-1}.K^{-1}], its section factor [m^{-1}].

VALIDATION

The developed models are validated against results of experimental tests performed in Ulster and results of FDS7[,8] simulations performed in the scope of a parametrical study.

Experimental tests

A series of 59 tests were conducted with different columns cross sections, with or without ceiling and several fire sources (fuel used, position and shape), as shown on Figure 14. A more accurate description of the setup and a detailed analysis is available in 1 and 9. These tests were also used to calibrate the CFD model used for the parametrical study1[,10].

Figure 14 : experimental setup and scheme of the setup

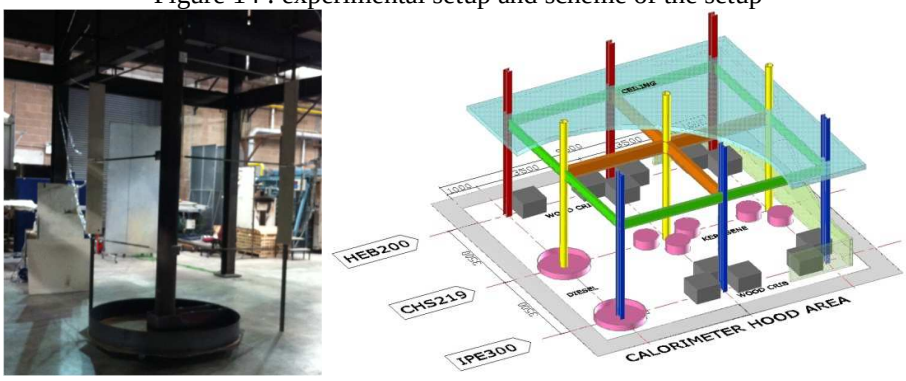

Initially, two solid flame shapes were envisaged: cylinder and cone. The results are displayed here for

these two shapes. The tests results are grouped depending on the location of the pans. Though many experimental configurations were investigated only the case with one pan of 0.7 m diameter is presented here, others are available in 1.

Two gauge positions and two pan locations are considered as indicated in Figure 15. The mean values are compared to those calculated by the model and reported in Table 1.Using the cylindrical flame shape, heat fluxes are always overestimated. On the opposite side, there is a rather good agreement if the solid flame has a conic shape.

Figure 15 : Relative position pan – gauge for a 1 m away pan (left) and for a 0.5m away pan (right)

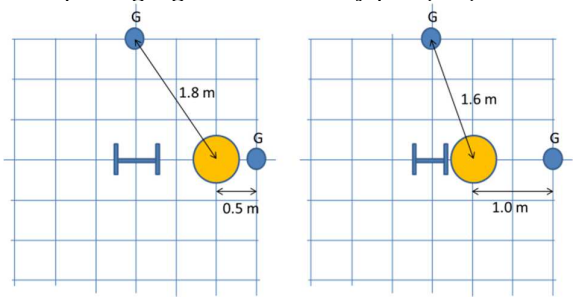

Table 1 : Comparison experiment – Model (1 pan)

Gauge location		Experiment mean	Cylinder flame	Conic flame
Height	Distance			
m	m	kW/m²	kW/m²	kW/m²
1.0	0.5	30.61	74.00	39.00
1.0	1.0	13.78	33.20	17.95
1.0	1.6	5.86	15.50	8.51
1.0	1.8	4.17	10.80	5.97
2.0	0.5	6.18	22.00	5.88
2.0	1.0	4.51	14.12	5.51
2.0	1.6	3.01	8.83	4.11
2.0	1.8	2.31	6.70	3.27

Numerical parametrical study

The aim of the parametrical study is confirming the good predictions of the analytical model when considering a conical flame shape and to extend it to cases with wide fire diameters. The analysis is divided into two parts: outside and inside the smoke layer. Furthermore, comparisons are performed for 3 versions of the model: the method with cylindrical flame shape (referred as Cylinder (int. meth.)), the method with conical flame shape (referred as Cone (int. meth.)) and the simplified method with a conical flame shape (referred as Cone (ana. meth.)).

The simulations are grouped in four sets, in each set the ceiling height is varying:

- Group 1: heat release rate of 500kW/m² and 4 m diameter pan,
- Group 2: heat release rate of 500kW/m² and 8 m diameter pan,
- Group 3: heat release rate of 1000kW/m² and 4 m diameter pan,
- Group 4: heat release rate of 1000kW/m² and 8 m diameter pan.

The radiative heat flux is measured at several heights and distances from the pan centre.
Outside the smoke layer, the radiative heat fluxes measured for groups 3 are displayed on

Figure 16 where the dash-dotted line corresponds to the pan radius. The agreement is excellent with a conical flame shape for both levels of complexity of the simplified model.

Figure 16 : Radiative heat flux at different heights for the case 1000kW/m² and 4m pan

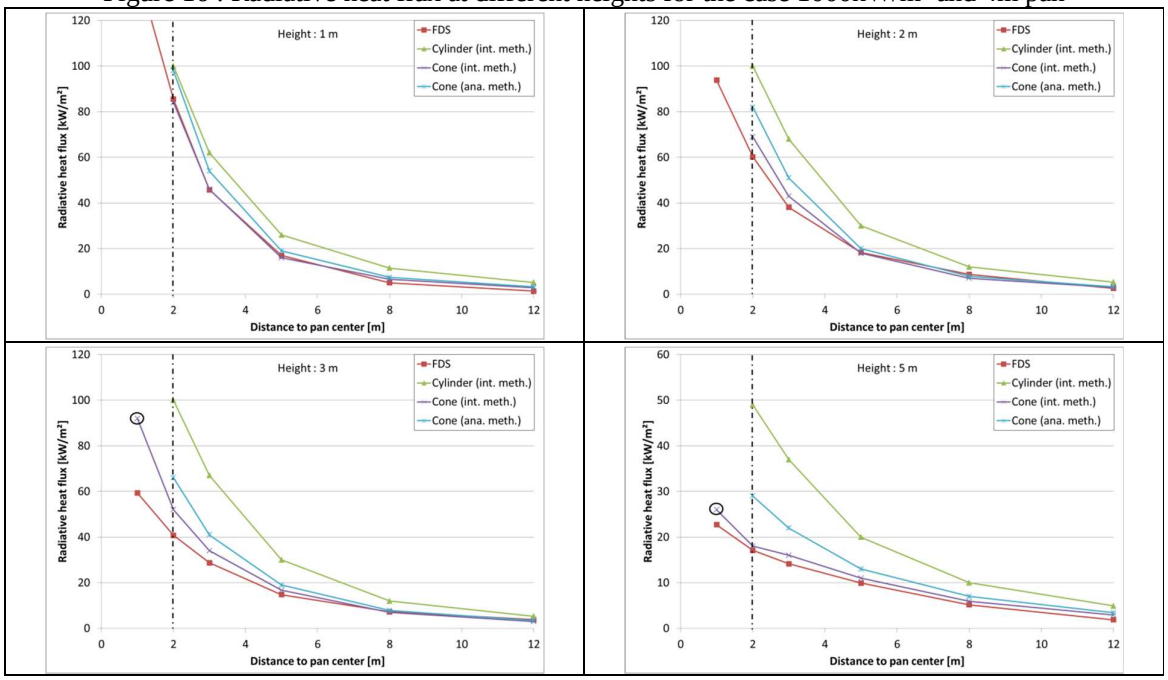

Inside the smoke layer, numerical simulations show that the received heat fluxes are identical for vertical and horizontal members. Therefore, it is consistent to use the same method to calculate the heat flux inside the smoke layer (under the ceiling), independently of the member orientation. Figure 17 shows that results are very close using the main method and the simplified one. This result was expected because the radiative and convective parts are calculated in the main method through a temperature based on Hasemi's heat flux. Furthermore, as soon as the ceiling height increases, the heat fluxes are strongly reduced and Hasemi gives an excellent agreement with FDS values independently of the fact that the flame is spreading under the ceiling or not. This is an important result because it shows that Hasemi method can be used even if the flame does not touch the ceiling.

Figure 17 : Heat flux under the ceiling for the case 500 kW/m² and 4 m pan

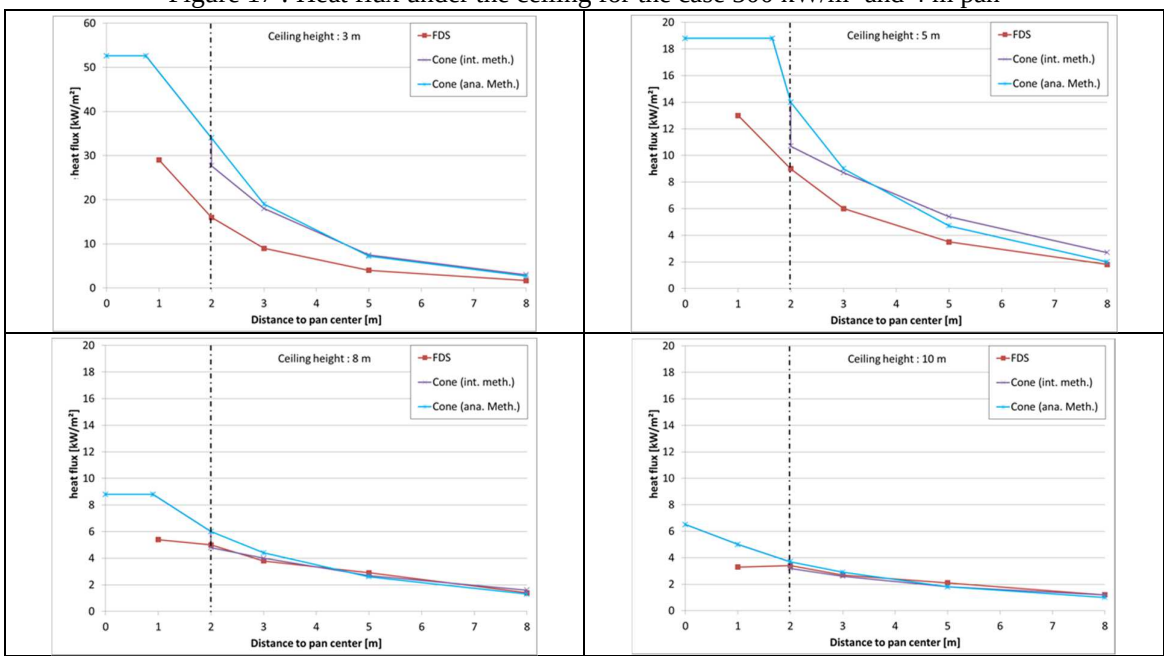

CONCLUSION

The model presented in this paper is based on the concept of virtual solid flame and allows assessing heat fluxes received by a vertical member. An emphasis is given to the radiative part which is more important for a vertical member submitted to a localised fire. The main equations used to determine the properties of the flame are based on well-known correlations used in fire safety engineering and, for some of them, already integrated into the Eurocodes. Several refinements are proposed, allowing a variable degree of complexity for the use of the model: it ranges from the use of numerical integration of some formulae to the use of equivalent or simplified analytical formulae. The comparison between the method, the experimental tests and CFD simulations shows a good agreement.

ACKNOWLEDGEMENTS

This work was carried out with a financial grant from the Research Fund for Coal and Steel of the European Community, within the LOCAFI project: "Temperature assessment of a vertical steel member subjected to localized fire", Grant N0 RFSR-CT-2012-00023.

REFERENCES

[1]O. VASSART, F. HANUS, J.-M. FRANSSEN, D. PINTEA, R. ZAHARIA, B. ZHAO, C. THAUVOYE, A. NADJAI, "Temperature assessment of a vertical steel member subjected to LOCAlised FIre", European research project, 2012-2015.

[2]NF EN 1991-1-2, Eurocode 1 — Actions on structures — Part 1-2 : General actions — Actions on structures exposed to fire, 3rd issue 2012.

[3]G. HESKESTAD, Luminous heights of turbulent diffusion flames, Fire safety journal, Vol 5 n°2, 1983.

[4]T. WAMATSU, Y. HASEMI et al, Experimental study on the heating mechanism of steel beam under a ceiling exposed to a localized fire, Asiaflam's 95, Hong Kong, 1995.

[5]J.-M. FRANSSEN, SAFIR: A thermal/structural program for modeling structure under fire, Engineering Journal, American Institute of Steel Construction Inc, Vol 42(3), 143-158, 2005.

[6]R. SIEGEL, J. R. HOWELL (1981), Thermal radiation heat transfer. Second Edition, Hemisphere Publishing Corporation, New York.

[7]K. Mc GRATTAN, K. Mc DEMOTT, S. HOSTIKKA., J. FLOYD, Fire Dynamics Simulator (Version 5) - User's Guide, National Institute of Standards and Technology, Special Publication 1019-5, October 2010.

[8]K. Mc GRATTAN, K. Mc DEMOTT, S. HOSTIKKA, J. FLOYD, Fire Dynamics Simulator (Version 5) – Technical Reference Guide – Volume 3 : Validation, National Institute of Standards and Technology, Special Publication 1018-5, October 2010.

[9]A. NADJAI, H. SANGHOON, O. VASSART, O. RENATA, Localised fire tests on the steel columns for different cross section and ceiling conditions., IFireSS-2015 International Fire Symposium, University of Coimbra, 20-23 April, 2015.

[10]N. TONDINI, F. HANUS, A. NADJAI and J.-M. FRANSSEN, Numerical analysis of hydrocarbon pool fire tests, Proceeding of the 1st International Conference on Structural Safety under Fire & Blast, Glasgow, UK, 2-4 September, 2015.